Design and fabrication of a compact multimode interference splitter with silicon photonic nanowires

Jingtao Zhou (周静涛)*, Huajun Shen (申华军), Huihui Zhang (张慧慧), and Xinyu Liu (刘新宇)

Institute of Microelectronics, Chinese Academy of Sciences, Beijing 100029, China

**E-mail: rapperr@live.cn*

Received December 16, 2008

A compact multimode interference (MMI) splitter with silicon photonic nanowires on silicon-on-insulator (SOI) substrate is designed and fabricated. The footprint of the MMI section is only approximately 3×10 (μm). The simulation results show that the device may have a low excess loss of 0.04 dB. The transmission loss of the silicon photonics wire is measured to be 0.73±0.3 dB/mm. The compact size and low transmission loss allow the device to be used in ultra-compact photonic integrated circuits. The device exhibits a good light splitting function. In a spectral range of 1549–1560 nm, the excess loss is 1.5 dB and the average imbalance between the two channels is 0.51 dB.

OCIS codes: 230.1360, 230.7370, 230.7380.

doi: 10.3788/COL20090711.1041.

Multimode interference (MMI) devices are extensively used in photonic integrated circuits (PICs) for light splitting and combining[1]. They have many advantages, such as wide optical bandwidth, polarization independence, simple structure, large fabrication tolerance, and small footprint. These outstanding advantages make them suitable for realizing various optical devices, such as multiport beam splitters, couplers[2], and switches[3]. Although beam splitters based on photonic crystals[4] may have even more compact sizes, their bandwidths are limited and polarization independence cannot be obtained.

Silicon-on-insulator (SOI) is a prominent platform for monolithical integration with electronic circuits. Because of the ultrahigh refractive index contrast between Si and SiO_2, extremely small devices, such as submicron nanowires[5] and photonic crystal waveguides[6], can be fabricated on SOI substrates. Silicon nanowires have a submicron cross-section and support single-mode propagation of light. They can confine light in a small cross-section, and guide it with low loss through sharp bends with radius of only several microns.

The 1×2 MMI splitters are extensively used as optical splitters and combiners in planar PICs. They often have a two-dimensional (2D) planar structure, consisting of one MMI waveguide, one input port, and two output ports. Ridge waveguides are often used to connect the input and output ports. However, owing to the large-size cross-section and requirement of large radius bends for low loss propagation of the ridge waveguide, MMI splitters with ridge waveguide usually have a large footprint, which limits their use in ultra-compact PICs. The adoption of silicon nanowires in connecting with input and output ports may greatly reduce the footprint of MMI splitters. The small footprint will help in the extensive application of the devices in ultra-compact integration of PICs. In this letter, the self-imaging principle is reviewed. Based on the restricted interference condition, the size of the MMI is further reduced. The MMI waveguide is simulated by RSoft's BeamPROP.

The operation of a MMI device is based on the so-called self-imaging principle[1,7]. Self-imaging is a property of multimode waveguide by which an input field profile is reproduced in single or multiple images at periodic intervals along the propagation direction of the waveguide. The length of a rectangular MMI region is usually $L_{\mathrm{MMI}} = p \times (3L_\pi)$, where $p = 1,2,\cdots$ (to minimize the size of MMI, usually $p = 1$), L_π is the coupling length of the two lowest-order modes,

$$L_\pi = \frac{\pi}{\beta_0 - \beta_1} = \frac{4nW_{\mathrm{e}}^2}{3\lambda}, \tag{1}$$

where n is the effective refraction index of the waveguide, β_0 and β_1 are the propagation constants of the lateral mode 0 and mode 1, and W_{e} is the effective width which takes into account the (polarization-dependent) lateral penetration depth of each mode field, associated with the Goos-Hahnchen shifts at the ridge boundaries. For high refractive index contrast waveguides, $W_{\mathrm{e}} \approx W_{\mathrm{MMI}}$, and W_{MMI} is the width of the MMI region. Thus we can obtain

$$L_{\mathrm{MMI}} = 3pL_\pi = \frac{3p\pi}{\beta_0 - \beta_1} \approx \frac{4npW_{\mathrm{MMI}}^2}{\lambda}. \tag{2}$$

This means that when W_{MMI} is reduced, L_{MMI} may decrease greatly. There is another way to further reduce the size of the MMI splitter. As mentioned above, the length of the MMI region should be $L_{\mathrm{MMI}} = p \times (3L_\pi)$ at general interference condition; no restrictions have been placed on the modal excitation. When the restrictions of the symmetry and the port location have been added to the input field, only some of the guided modes in the multimode waveguide are excited; this is the so-called restricted interference condition. At the restricted interference condition, the length periodicity of the mode phase will be reduced several times. For example, when an symmetric input field $\varphi(y, 0)$ (for example, a Gaussian beam) is launched at the central position, only the even symmetric modes are excited; single images of the input field $\varphi(y, 0)$will now be obtained at

$$L = p \times \left(\frac{3}{4}L_\pi\right), \text{with } p = 1, 2, \cdots. \tag{3}$$

The imaging is obtained by linear combinations of the (even) symmetric modes, and the mechanism will be called symmetric interference. N-fold images can be obtained[1] at distances

$$L_0 = \frac{p}{N} \times \left(\frac{3}{4} L_\pi\right), \text{with } p = 1, 2, \cdots. \tag{4}$$

The images of the input field $\varphi(y, 0)$ are symmetrically located along the y-axis with equal space W_{MMI}/N.

Optical N-way splitters can, in principle, be realized on the basis of the general N-fold imaging at lengths given by Eq. (4). However, by exciting only the even symmetric modes, l-to-N beam splitters can be realized with multimode waveguides that are four times shorter[1]. The 1×2 waveguide splitter/combiner is perhaps the simplest MMI structure ever realized; it needs only two symmetric modes. Here, we will discuss the simulation and design of an ultra-compact 1×2 MMI waveguide splitter used as a 3-dB beam splitter, with silicon photonic nanowires serving as input and output ports.

In this case, $n = 3.45$ (the refractive index of silicon), $\lambda = 1.55$ μm. Assuming $W_{\mathrm{MMI}} = 3$ μm, and substituting them into Eq. (2), we can get

$$L_\pi \approx \frac{4nW_{\mathrm{MMI}}^2}{3\lambda} = 26.71\ \mu\mathrm{m}. \tag{5}$$

Substituting Eq. (5) and $p = 1$, $N = 2$ into Eq. (4), we can get

$$L = \frac{p}{N} \times \left(\frac{3}{4} L_\pi\right) = 10.02\ \mu\mathrm{m}. \tag{6}$$

Since the width of MMI region $W_{\mathrm{MMI}} = 3$ μm, the distance between the two output ports is $W_{\mathrm{MMI}}/2 = 1.5$ μm; they are symmetrically located at $y = \pm 0.75$ μm.

The MMI splitter was designed to perform a 3-dB waveguide splitter. The simulation tool of Rsoft's BeamPROP based on the beam propagation method was used to analyze the coupling efficiency and optimize the device performance. Figure 1(a) is the schematic illustration of the MMI splitter. Figure 1(b) shows the calculated fundamental mode with TE polarization, which is launched into the input silicon photonic nanowire. The cross-section of silicon photonic nanowire is 0.54×0.26 μm.

As mentioned above, L_{MMI} is in direct proportion to W_{MMI}^2, that means, when W_{MMI} is reduced, the length of a rectangular MMI region L_{MMI} can be greatly decreased, and thus the miniaturization of the MMI devices

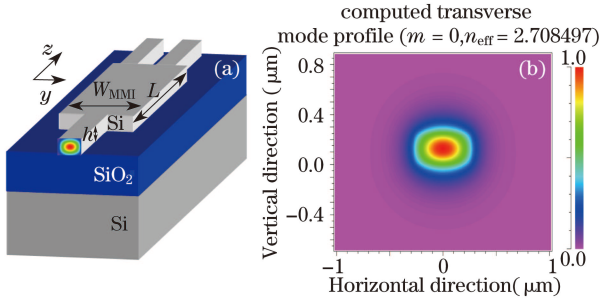

Fig. 1. (a) Schematic illustration of the MMI splitter; (b) launched TE polarization optical mode profile.

Table 1. Number of Excited Modes N and Width of the Gap W_{gap} under Different W_{MMI}

W_{MMI} (μm)	3.5	3	2.5	2	1.5
N	8	7	6	5	4
W_{gap} (μm)	1.21	0.96	0.71	0.46	0.21

can be realized. However, W_{MMI} cannot be reduced too much, because the multimode waveguide must be designed to support a large number of transverse modes (typically >3)[1]. These modes can be excited and can interfere with each other, and thus the N-fold images can be obtained. Under different widths of multimode waveguides, the maximum number of excited transverse mode N and the width of the gap between the inner edges of the two output nanowires are listed in Table 1. According to the self-imaging principle, the spacing between the two output ports will be $W_{\mathrm{MMI}}/2$, and thus the gap is obtained as

$$W_{\mathrm{gap}} = W_{\mathrm{MMI}}/2 - w, \tag{7}$$

where w is the width of the output waveguides.

Further reducing W_{MMI} to 1.5 μm, the more compact device may be obtained. However, the narrow gap between the two waveguides is hard to control accurately. Compromising all the factors, the width of the multimode waveguide was set at 3 μm. The maximum number of the excited transverse mode N and the width of the gap between output waveguides are given when a different width of the MMI waveguide is chosen.

To further optimize the device performance, a parameter scan of the MMI output location along the y-axis was performed at a step of 0.01 μm and the output power of one port was monitored. The origin of the y-axis was set at the center of the MMI waveguide, and the output nanowires were symmetrically located at both sides of the origin. The device height was fixed at 0.26 μm. The simulation result is shown in Fig. 2. From the figure, the optimized output location can be obtained at ±0.79 μm, and it is consistent with what has been deduced from the self-imaging principle ($y = \pm 0.75$ μm). Furthermore, we fixed the output location at ±0.79 μm and performed a parameter scan of the MMI's length at a step of 0.1 μm and monitored the output power of one output port. Figure 3 shows that the optimized length of the MMI section is 9.58 μm, which is also consistent with the results deduced from the self-imaging principle ($L = 10.02$ μm). The maximum output power is 0.495 in each output port and the total output power is 0.99 (the launched power is set to 1), which shows a low excess loss of 0.04 dB. Figure 4 shows the lateral optical power distribution in the MMI section ($y = \pm 0.75$ μm; $L = 9.58$ μm). The self-images are reconstructed at the output ports with equal splitting power (0.495).

The fabricating technology of the MMI splitter was borrowed from the silicon microelectronics industry. We have used commercially available SOI wafers with a top silicon thickness of 0.26 μm and a buried oxide layer of 1 μm from Soitec Company. In the fabricating process, JBX6300FS electron beam lithography (EBL) system and Corial 200IL inductively coupled plasma (ICP) etcher were used to perform the lithography and etching process.

Figure 5 shows the cross-section of the silicon photonic nanowire. The cross-section exhibits a rectangular shape and the bottom angle of the sidewall is 86°, while the size in the cross-section is 0.51×0.26 (μm). Compared with the design, the width of the nanowire has a little deviation caused by the variation in the fabricating process.

Figure 6 shows the transmission loss of the silicon photonics nanowire using the Fabry-Perot (FP) fringe contrast measurement method[8]. A group of nanowires with different lengths have been made. Each nanowire can be treated as a FP cavity, which consists of two interfaces with the same reflectivity R and

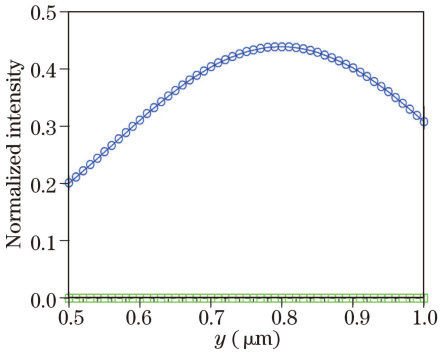

Fig. 2. Optimization of device performance by considering output power versus MMI output location in the y-axis direction. The origin of y-axis is the middle of the MMI waveguide.

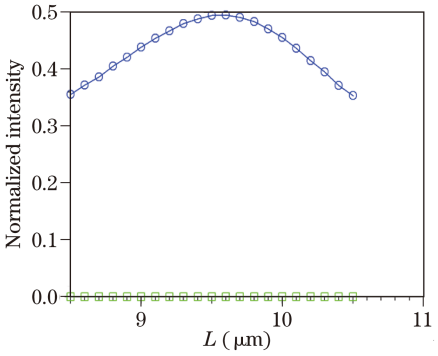

Fig. 3. Optimization of device performance by considering output power versus MMI length L.

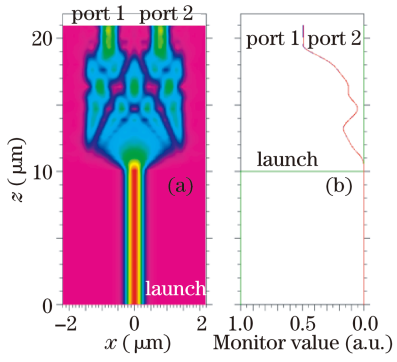

Fig. 4. Simulation of the optimized structure of a MMI splitter. (a) Optical power distribution in the MMI section; (b) power monitored at each port.

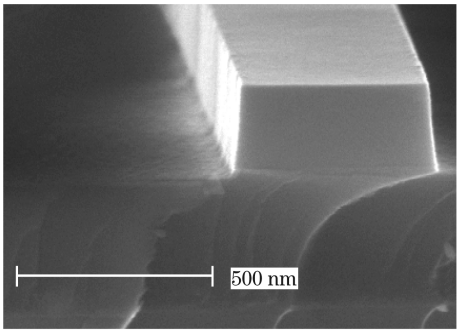

Fig. 5. SEM micrograph of the cross-section of silicon photonics wire.

a medium with loss τ^2. We can use its typical transmission spectrum to determine the losses inside the cavity. Figure 6(a) shows the transmission spectrum when the length of the nanowire is set at 0.1 mm.

$$\Delta I(\mathrm{dB}) = I_{\max} - I_{\min}, \tag{8}$$

$$S = 10^{\frac{\Delta I}{10}}, \tag{9}$$

$$R\tau^2(\mathrm{dB}) = 10\log\frac{\sqrt{S}-1}{\sqrt{S}+1}, \tag{10}$$

where $I_{\max}$ and $I_{\min}$ are the maximum and minimum output powers, respectively. According to Eqs. (8)–(10), $R\tau^2$ is extracted from the FP cavity transmission spectrum rather than the measured power and has a linear relationship with the length of nanowire L_{pw} as

$$R\tau^2(\mathrm{dB}) = -\frac{10R}{\ln 10}\alpha_{\mathrm{pw}}L_{\mathrm{pw}} + B, \tag{11}$$

where α_{pw} is the propagation loss of the nanowire, L_{pw} is the length of the nanowire, and B is a constant. We can measure the value of ΔI, and then obtain $R\tau^2$ at different L_{pw}. Figure 6(b) shows the linear relationship between $R\tau^2$ and L_{pw}. Finally, the propagation loss of the silicon photonic nanowire $\alpha_{\mathrm{pw}} = 0.73 \pm 0.3$ dB/mm can be obtained from the slope of the curve. By using this method, the repeatability and precision of the measurement are greatly improved.

The scanning electron microscopy (SEM) picture of the fabricated MMI splitter is shown in Fig. 7(a), and the enlarged photo of the device output port is shown in Fig. 7(b). As can be seen in Fig. 7(a), the size of the MMI region is approximately only 3×10 (μm). The width of the MMI waveguide is 2.86 μm, which is a little less than the expected value. This deviation can be cancelled by enlarging the width in the layout design to compensate for the width reduction caused by etching. The location of the output nanowires is quite precise.

The MMI splitter is usually characterized by excess loss and imbalance. The excess loss is defined as the difference between the sum of the powers exiting from the output ports and the power entering the input port for the MMI section. The imbalance of an $N \times M$ splitter is defined as the maximum-to-minimum output power ratio for all M outputs, expressed in decibels.

For device measurements, an automatic alignment system based on Newport PM500-C precision motion controllers was used for precise alignment. A single-mode lens fiber was used to couple light into the polished end

facet of the access waveguide. The light transmitted through the sample was collected by another lens fiber and projected on a power detector. The input optical power was fixed to 0 dBm to normalize the output power. In order to estimate the excess loss, a straight reference waveguide with the same couplers and the same length of nanowire was fabricated and measured. Through the automatic alignment system, precise and repeatable measurement can be performed. Thus we assume that the MMI splitter has the same coupling and transmission losses as the reference waveguide, and the difference between them is the excess loss of the MMI splitter. Figure 8 shows the total output power of the device; the fit curve and the output power of the reference waveguide are also given. The wavelength of the light is swept from 1549 to 1560 nm. The average excess loss is obtained to be 1.5 dB in a spectral range of 1549–1560 nm. The discrepancy between the simulated result and the measured result may be caused by the variations in the processes and the errors in the measurement. In Fig. 8, the oscillation amplitude of the MMI splitter is slightly lower than that of the referenced waveguide, hence, the existence of the MMI region may reduce the FP cavity effect.

Figure 9 shows the imbalance of the two output ports. A maximum value of 2.50 dB appears at 1549 nm. The average imbalance is 0.51 dB in the range of 1549–1560 nm. The imbalance between the two output ports was caused by the unperfect symmetry introduced by process variations. Strict fabrication processes and more accurate design with proper process tolerance may further improve the performance of the MMI splitter.

In conclusion, a compact MMI splitter with silicon photonic nanowires on SOI substrate is designed and fabricated. The footprint of the MMI section is approximately only 3×10 (μm). The simulation results show that the device may have a low excess loss of 0.04 dB. The transmission loss of the silicon photonics wire is measured to be 0.73±0.3 dB/mm. The device exhibits a good light splitting function. In a spectral range of 1549–1560 nm, the excess loss is 1.5 dB and the average imbalance between the two channels is 0.51 dB. The compact size and the low excess loss allow the device to be used in ultra-compact PICs. Strict and accurate control in the fabrication process may improve the performance of the MMI splitter and help its application in ultra-compact integration of PICs.

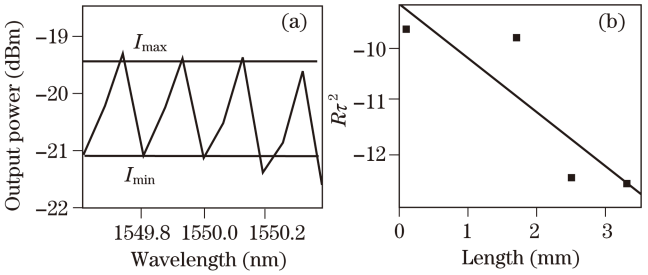

Fig. 6. (a) Transmission spectrum when the length of the nanowire is set at 0.1 mm; (b) linear relationship between $R\tau^2$ and the length of nanowire L_{pw}.

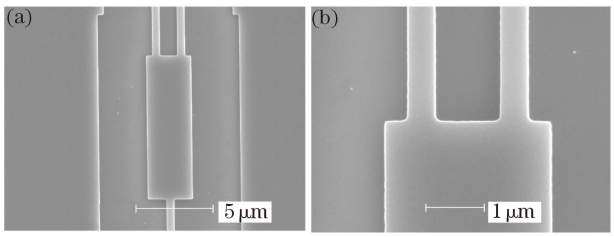

Fig. 7. (a) SEM micrograph of the MMI waveguide splitter; (b) enlarged photo of the device output port.

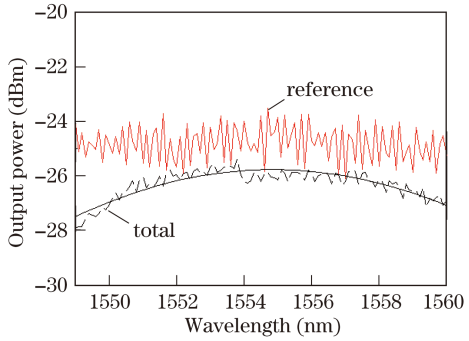

Fig. 8. Output optical power versus the wavelength of the incident light. The solid curve represents the fit curve of the total output power.

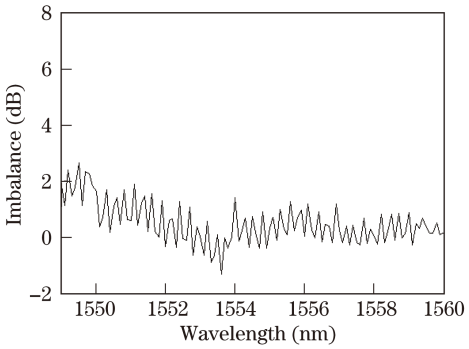

Fig. 9. Imbalance between the two output ports versus the wavelength of the incident light.

The authors acknowledge Prof. Ke Wei for his very useful suggestions and Engineer Xing Bo for his help with the device measurement.

References

1. L. B. Soldano and E. C. M. Pennings, J. Lightwave Technol. **13,** 615 (1995).
2. K. Solehmainen, M. Kapulainen, M. Harjanne, and T. Aalto, IEEE Photon. Technol. Lett. **18,** 2287 (2006).
3. X. Jia, S. Luo, and X. Cheng, Opt. Commun. **281,** 1003 (2008).
4. Y. Shen, J. Sun, X. Shen, J. Wang, L. Sun, K. Han, and G. Wang, Chin. Opt. Lett. **6,** 709 (2008).
5. Y. A. Vlasov and S. J. McNab, Opt. Express **12,** 1622 (2004).
6. Y. Huang, X. Mao, C. Zhang, L. Cao, K. Cui, W. Zhang, and J. Peng, Chin. Opt. Lett. **6,** 704 (2008).
7. S. Liao, M. Gong, and H. Zhang, Chinese J. Lasers (in Chinese) **35,** (suppl.) 115 (2008).
8. W. Bogaerts, "Nanophotonic waveguides and photonic crystals in silicon-on-insulator" (in Dutch) PhD Thesis (Ghent University, Ghent, 2004).